

# Hot-spot Selection and Evaluation Methods for Whole Slice Images of Meningiomas and Oligodendrogliomas\*

Zaneta Swiderska, Tomasz Markiewicz, Bartłomiej Grala, and Janina Słodkowska

**Abstract**— The paper presents a combined method for an automatic hot-spot areas selection based on penalty factor in the whole slide images to support the pathomorphological diagnostic procedure. The studied slides represent the meningiomas and oligodendrogliomas tumor on the basis of the Ki-67/MIB-1 immunohistochemical reaction. It allows determining the tumor proliferation index as well as gives an indication to the medical treatment and prognosis. The combined method based on mathematical morphology, thresholding, texture analysis and classification is proposed and verified. The presented algorithm includes building a specimen map, elimination of hemorrhages from them, two methods for detection of hot-spot fields with respect to an introduced penalty factor. Furthermore, we propose localization concordance measure to evaluation localization of hot spot selection by the algorithms in respect to the expert's results. Thus, the results of the influence of the penalty factor are presented and discussed. It was found that the best results are obtained for 0.2 value of them. They confirm effectiveness of applied approach.

## I. INTRODUCTION

The quantitative examination of histological tissues subject to immunostain tests is a basic method of recognizing a tumor, the choice of optimal therapy and defines the prognostic indicators. One of the most important marker is the proliferation marker Ki-67/MIB-1 in central nervous system tumours. Especially, in meningiomas and oligodendrogliomas (the most frequent primary intracranial tumour) the proliferation index differentiating them into meningothelial (WHO I), atypical (WHO II), anaplastic (WHO III), and oligodendrogliomas WHO II and (III), and correlate with tumour recurrences [1,2]. The quantitative evaluation of tumor proliferation based on selection of a set of high power field of view. For each of them the immunopositive cell nuclei marked with a brown color and immunonegative cell nuclei marked blue have to be counted to establish the Ki-67 index. When a lot of algorithms for cell segmentation and counting in the images are described in the literature [3,4], the approaches to hot spot finding in the whole slide images are still under design. The most of them are addressed to an analysis of tissue treated in a standard Hematoxiline & Eosine stain [5,6]. Recently, the algorithm for microvessel analysis we can found in the paper [7] and in

[8] the authors present method for the increasing of visibility of the positive nuclei at low resolution image. However, still the hot spot fields are selected manually. In the other recently presented paper [9] the automated selection of hot spots algorithm was proposed. The adaptive step finding technique has been applied for the increasing the computational efficiency and performance of hot spot detection. Despite significant progress, a problem of the spatial distribution of the selected hot spot fields was not taken into account in this paper. As far as we know, algorithm containing hotspot selection and problem of the hot spot spatial distribution, for whole slice image, not yet been presented in the literature.

In routine diagnostic practice, representative hot-spot areas are manually selected by histopathologists using visual examination of Ki67-immuostained specimen at a low magnification. This process might lack reproducibility and affect the Ki-67 due to subjectivity of evaluation [10,11]. The influence of many factors, such as the expert's experience, fatigue, previously viewed preparations and external factors are the most significant. Also, the histological criteria of a hot spot selection are flexible. The selected fields should represent the areas of the high Ki-67 index, but also different tumor localization. In this paper we propose and apply the mathematical morphology based algorithms to estimate the number of immunopositive cells and selection of the high Ki-67 fields. The additional problem in the whole slide examination is also the occurrence of areas of hemorrhages, which are also stained with brown. Therefore, there is a need to differentiate them from the areas of tumor proliferation. The texture analysis and classification can be useful in the aspect of analysis and recognition of the whole structure (pattern) of the tissue. Based on these tools we eliminate hemorrhages from the specimen map. Finally, to diversification of the selected localizations we propose the artificial model of this process with a penalty function to increase spatial distribution of the hot spots. The measure of concordance between the manually and automatically selected hot spot fields was also proposed.

## II. METHODS

### A. Material and image acquisition

Fifteen cases of meningiomas and oligodendrogliomas subject to Ki-67/MIB-1 immunohistochemical staining were obtained from the archives of Department of Pathomorphology from the Military Institute of Medicine in Warsaw, Poland. The data collection was approved by the IRB of the Military Institute of Medicine. Acquisition of the whole slide images was performed on the Aperio ScanScope scanner. The images were acquired under magnification 400x with a resolution 0.279  $\mu\text{m}$  per pixels. Due to a very large size of images in the contextual analysis of the

\* Research supported by the National Centre for Research and Development (PBS2/A9/21/2013 grant), Poland.

Z. Swiderska is with the Warsaw University of Technology, Warsaw, Poland (phone: +48222347235; fax: +48222345642; e-mail: swidersz@ee.pw.edu.pl).

T. Markiewicz is with the Warsaw University of Technology, and the Military Institute of Medicine, both Warsaw, Poland (e-mail: markiewt@iem.pw.edu.pl).

B. Grala and J. Słodkowska are with the Military Institute of Medicine, Warsaw, Poland (e-mail: bgrala@wim.mil.pl, jsłodkowska@wim.mil.pl).

specimen it was necessary to reduce the resolution to enable direct examination and visualisation. We have chosen eight-fold reduction of the resolution to enable the evaluation performed both manually and by a computer.

### B. Tumor map for hot spot selection

The original whole slide image is not adequate to directly defining the hot spot fields. It contains not only the tumour lesion, but also free-tissue areas and especially stained artefacts such as a hemorrhage. The proliferative Ki-67 index can be significantly overestimated if the hemorrhage areas are processed like hot-spot areas. Thus, the establish of specimen map for the hot spot selection is necessary. It can be realized in two steps: a) defining a map of specimen, b) elimination of the areas containing blood cells (hemorrhages).

The map of specimen is produced by using the thresholding procedure and morphological filtering [12]. To start with, an image produced by the morphological operation of opening is subjected to brightness equalization. It is performed using a structuring element shaped as a disc with a large beam (100 pixels). The operation expressed in the form (1) is performed independently for every RGB colour components.

$$f = f / \Theta_{SE}^f \quad (1)$$

Afterwards, differencing image B and R components is processed with Otsu thresholding method [13]. Morphological operations such as: erosion, dilatation, fill holes are conducted on the resulting image. Small areas are eliminated from final specimen map in order to remove the unnecessary part of image. This reduces the number of operations and shorten the time of image processing.

The differentiation of the tumour with hemorrhage areas is solved using the texture analysis and classification. Our approach to texture analysis is based on the normalized probability applied to the pixel intensity of the image. We use the modified formulas of Unser features [14] to a local feature description. The defined textures were determined for each of the components in the RGB, CMYK colour spaces, and for the combined  $u$  (from CIE Luv) and  $C$  (from CMYK) representation. The latter representation unifies the image description in the areas of tumour, and at the same time assumes lower values in the areas of blood. In this way we have determined 64 features as descriptors of the defined patterns in the classification process. Next, the Fisher's linear discriminant for the features was applied [15] to establish a set of 25 the most significant ones. Finally, the Support Vector Machine (SVM) with Gaussian kernel function [16] was applied as a classifier to recognize the hemorrhage areas. Thus, the result of this process was the tumor map.

### C. The algorithm of hot spot candidate detection

The accurate detection of immunopositive cells within the tumour area is a key step in the algorithm of hot-spot area localization. These fields correspond to areas with dense immunopositive reactions. We propose the two approaches, first (Algorithm I) based on colours

thresholding, and second (Algorithm II) based on mathematical morphology.

The Algorithm I based on thresholding of differential image of B and G colour components. In order to obtain the most adequate map of immunopositive cell nuclei, values of G component were multiplied by 0.85 factor before subtracting both components. Through this operation, only the brownish areas of the image receive value greater than zero. This calculation was restricted to the image regions covered by the tumour map. The next step is to threshold this image using the threshold value obtained by the Otsu method [13]. The purpose is to remove the components other than immunopositive cells, for example areas representing the colouration of stromal.

The Algorithm II based on the evaluation of the spatial relation of the stained brown objects to their neighboring environment. It is carried out by morphological operations performed on the component  $u$  of CIE Luv representation of colours after image transformation. This component is strictly associated with the red colour and it is the best for differentiating the immunopositive cells from the remaining part of the image. In order to detect objects with pixel intensity standing out significantly from the environmental components, the extended regional minima transformation was applied. The regional minima connecting pixels with a constant intensity value and whose external boundary pixels have a higher value, are detected. The key parameter of the extended regional minima transformation is the choice of  $h$  value, representing the criterion for the minimum difference between the intensity of the point in a local minimum and its close environment. This value was determined in an experimental way and was set on the level of 45.

Finally, for the isolated marks representing the immunoreactive tumour cells, a dense map was created. This map contains the spatial distribution of centers representing the immunopositive tumour cells.

### D. Hot spot selection with penalty factor

The selection of areas representing hot-spots is based on finding the local maxima with the highest density of immunopositive cell nuclei. The density map can be obtained, inter alia, by counting the number of objects in each window (field of view) or by averaging filter applied to the binary mask. In practice, it may happen that only one area of considerable dominance proliferative Ki-67 index occurs within the analyzed specimen. In such case an automatic quantitative analysis can lead to the selection of the hot-spot areas only in this particular region. However, one of the guidelines for quantitative assessment of tumour scan is to identify the fields for the analysis within multiple areas of tumour proliferation. In order to force the selection of the hot-spots in the entire scanned image, the penalty function is proposed and applied. This is a key step our developed algorithms. It associates the distance between the designated areas and position of another candidate for hot-spot. The distance map from the just selected hot spots with centres placed in  $(x_i, y_i)$  positions takes the value defined by the following formula

$$penalty = 1 - \rho \sum_i \frac{1}{\left(\sqrt{(x - x_i)^2 + (y - y_i)^2}\right)^{0.5}} \quad (2)$$

The increase of  $\rho$  value results in enforcing greater scattering of the designated areas. It should be selected experimentally, that it is presented in the result section.

The new density map with applying the penalty function was created by the multiplication of the received dense map by the map of distances. In the case where one hot-spot area is dominating, the penalty term allows to determine the hot-spot positions in different localizations of the tumour. As a result, the algorithm determines a set of hot-spot localizations representing high immunopositive reaction in diverse locations. The final analysis of Ki-67 index in these selections was performed on full resolution images with the help of the algorithm described in [4].

### E. Localization concordance measure

In the aim of evaluation localization of hot spot selection by the algorithms in respect to the expert's results, the localization concordance measure (LCM) was proposed. The localization concordance measure was calculated by the following formula:

$$LCM = \sum_i (w_i * \text{sigm}(\min_j \text{dist}[(x_j, y_j), (x_i, y_i)] / (4FOV_{size}))) \quad (3)$$

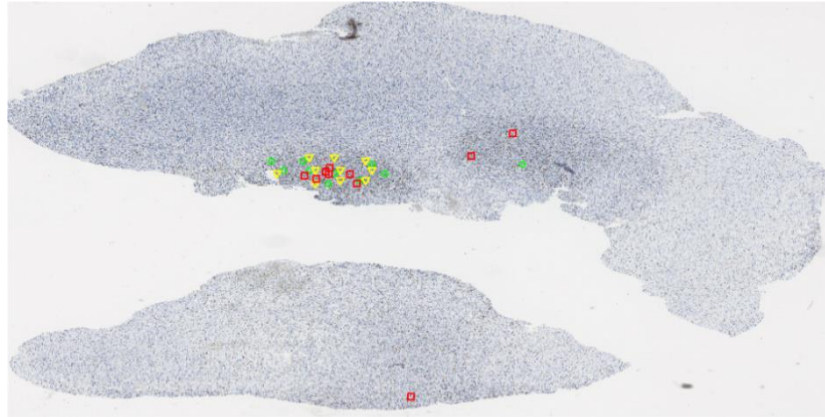
where :  $w_i = \frac{L_{E_i}}{L_E}$

in which:  $L_{E_i}$  - level of Ki-67 index for the expert in counted field,  $L_E$  - mean level of Ki-67 index for the expert, and  $FOV_{size}$  is a one field of view size. Low value of the LCM testifies to similar hot-spots localization selected by algorithm to expert's result. This mean, that the expert's selected fields are represented by the fields come from algorithm, e.g. represents this same tumour area. If expert and algorithm select fields of view from miscellaneous virtual slide area, then localization measure is high. The proposed measure allows evaluate the correctness of choice of hot spot fields, and also find the best penalty factor.

### III. RESULTS

Studies were conducted for fifteen cases of meningiomas and oligodendrogliomas. By the presented algorithms we determined twenty hot-spot fields in each scan and made their diagnostic evaluation by the quantitative analysis. The exemplary hot spot selection are present in the Fig. 1 with respect to an expert's result.

a)



b)

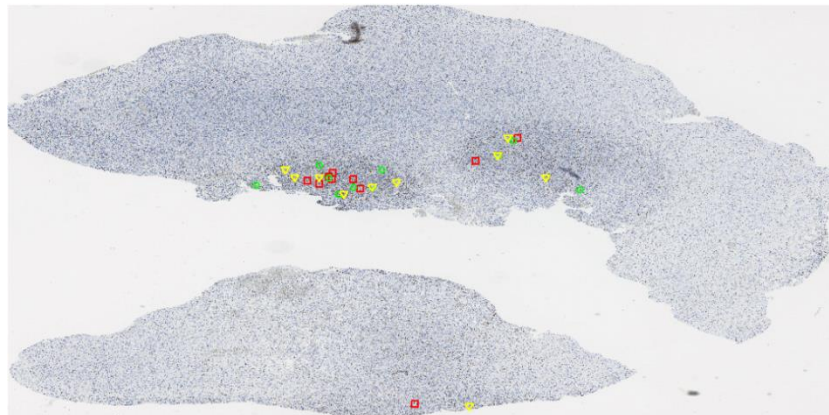


Figure 1. Virtual slide presenting the exemplary hot-spot selection marked by the Expert 1 ( $\square$ ), and hot-spots designated by the algorithms (Algorithm I- $\circ$ , Algorithm II- $\Delta$ ) for  $\rho = 0$  (a), and  $\rho = 0.2$  (b).

First, we analyzed the influence of penalty factor to hot spot selection and Ki-67 level return by the algorithm. The  $\rho$  value was examined in the range from 0 to 0.5. The zero value mean no penalty for a field concentration. The two exemplary hot spot selection for 0 and 0.2 values are present in the Fig. 1. As can see if the penalty function wasn't applied (Fig. 1a), all automatically selected hot spot fields are located in a one high proliferation region of tumour. If the penalty function was introduced, the selected fields represent different tumour areas with a better agreement with expert's result (Fig. 1b).

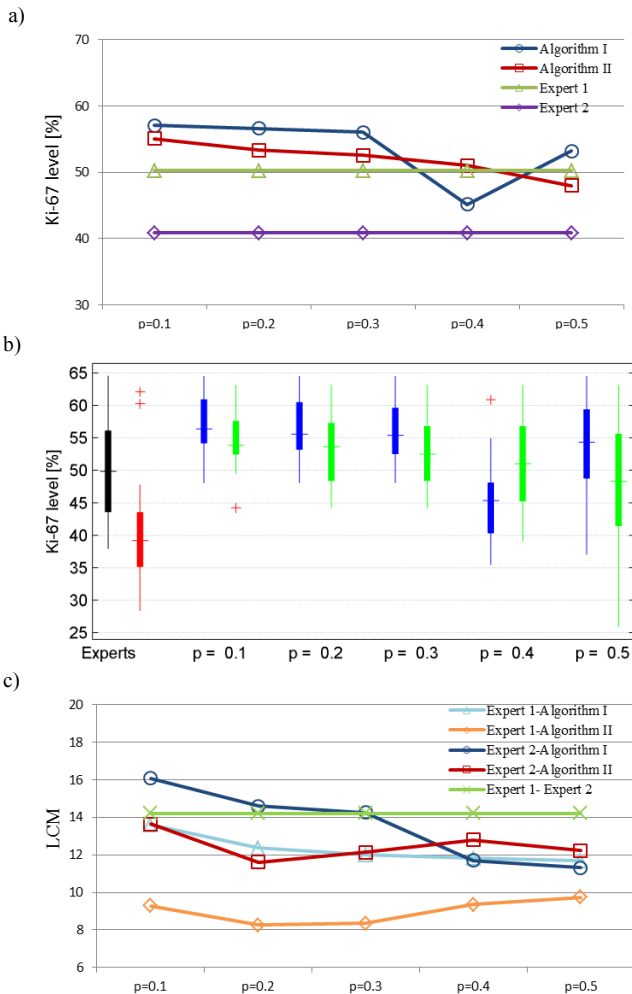


Figure 2. The results of analysis of a penalty factor influence, to the Ki-67 level (a) and variability (b) for both algorithms (I left and II right), and LCM for a one case (c)

Nevertheless, all selected regions are located in the higher proliferation areas of the specimens. The detailed quantitative analysis better explain the significance of these selections on the assessment of the analyzed material.

The analysis of a penalty factor influence to the Ki-67 level and variability, and LCM for a one case is presented in Fig.2.

The increasing of  $\rho$  value results:

- a lower Ki-67 level for both algorithms (Fig.2a),
- extension of the range of returned values for a set of hot spot fields (Fig. 2b),
- finding the best localization concordance with expert's results for about 0.2-0.3 value (Fig. 2c).

The study for three other cases (Fig. 3) shows that  $\rho$  value equals 0.2 has one of the best correlation between the localization concordance and maximal Ki-67 level. Thus, this value was applied in the further investigations.

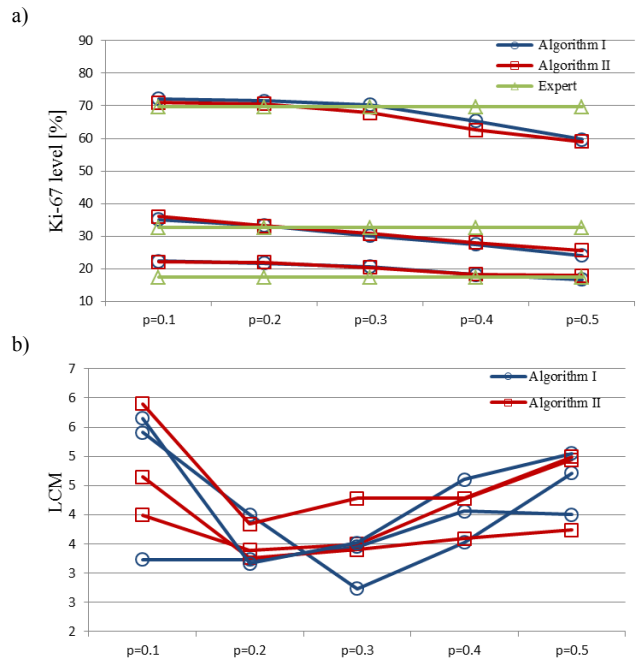


Figure 3. The results of analysis of a penalty factor influence, to the Ki-67 level, and LCM for three cases.

Finally, the analysis of a selection of 20 hot-spot fields in fifteen investigated cases was performed. The detailed results are presented in Table 1.

Table 1. The results of quantitative analysis of Ki-67 index and LCM in the designated fields of view for the hot-spot areas selected by the expert, and by the developed algorithms (algorithm I and algorithm II).

ID	Ki-67 %			LCM	
	Expert	Algorithm I	Algorithm II	Expert-Algorithm I	Expert-Algorithm II
1	15.79	19.67	20.72	9.70	12.12
2	50.24	56.60	53.35	12.36	8.27
3	41.09	50.37	42.32	5.41	7.36
4	25.82	35.01	33.24	9.00	6.89
5	17.52	21.74	21.94	3.23	3.26
6	26.45	24.86	27.25	4.77	4.27
7	11.16	12.25	12.81	5.92	8.26
8	22.36	22.48	26.24	9.76	6.71
9	69.72	71.48	70.62	4.00	3.40
10	22.87	22.05	24.85	3.87	2.95
11	48.96	44.86	48.02	8.29	6.18
12	18.93	20.81	22.65	7.61	8.52
13	32.58	33.23	33.19	3.17	3.84
14	11.53	11.24	13.38	6.48	6.73

15	3.06	3.85	4.94	7.29	7.66
<b>Mean:</b>	<b>27.87</b>	<b>30.03</b>	<b>30.37</b>	<b>6.72</b>	<b>6.43</b>

There exist some differences between the average values of Ki-67 index for the areas selected by expert and by the developed algorithms I and II. Both developed algorithm give higher Ki-67 result than expert's result. The LCM comparison shows that, fields selected by algorithm I and algorithm II reflect the tumour area selected by expert. Fields selected by developed algorithms were located in the similar tumour areas but they had the higher Ki-67 level, than results achieved by expert. The best results were achieved by Algorithm II, because level of the Ki-67 was highest, and at the same time the LCM was on low level. Our results confirm the advantage of automatic evaluation over the manual assessment.

#### IV. CONCLUSIONS

In the commercial market, there some product mainly development by the manufacture of scanners or cooperating companies, that there are addressed to the specific slide format and viewer. We can notices such solution as Genie (Aperio) [17], QuantCenter (3DHistech) [18], TissueStudio (Definiens) [19], and AxioVision (Zeiss) [20] which are capable of high quality image processing and Ki67 quantitation. Unfortunately, these products are not freely available for comparative testing. Thus, the assessment of their capabilities are restricted to a sales information. Basing on them we conclude, that the problem of simulating of the hot spot spatial distribution is still not resolved in the commercial solutions.

We have presented the effective method for an automatic localization of the hot-spot areas based on penalty factor in meningioma and oligodendrogliomas tumours. Two different approaches have been suggested. The results showed that applied  $\rho$  allows to achieved differentiated location of hot-spot selected. Moreover, we proposed localization concordance measure (LCM) for evaluation localization of hot-spot selection by the algorithms in respect to the expert's results. Based on LCM and Ki-67 index we compared and evaluated field selected by expert and developed algorithm.

Fields selected by both developed algorithms had higher the Ki-67 level than fields selected by expert, but the localizations was similar. In the case of manual selection of hot-spot areas by an expert, the considerable variability can be observed. This is mainly due to subjectivity of the image assessment, in particular when the image encompasses the considerable regions of high proliferation. The algorithm II has shown the advantage over the algorithm I in accurate detection of hot-spot areas. We conclude, that the algorithm II is more independent of colour intensity of immunohistochemical staining. The use of presented algorithms allows to select hot-spot fields with high Ki-67 index from miscellaneous localization. thanks this, we can evaluated different tumour areas.

The use of maps of specimen and the elimination of hemorrhage areas have reduced the size of an image under analysis and also the computational time. The presented

methods have good reproducibility (characterized by the repeatability of results) which gives them an advantage over the traditional, manual way of identification of hot-spot areas in meningioma and oligodendrogliomas.

#### REFERENCES

- [1] D. L. Commins, R. D. Atkinson, and M. E. Burnett, "Review of Meningioma Histopathology," *Neurosurg. Focus*, vol. 23, no. 4, pp. E3, October 2007.
- [2] A. Terzi, E. A. Saglam, A. Barak, and F. Soylemezoglu, "The significance of immunohistochemical expression of Ki-67, p53, p21, and p16 in meningiomas tissue arrays," *Pathol. Res. Pract.*, vol. 204, no. 5, pp. 305–314, May 2008.
- [3] Y. J. Kim, B. F. M. Romeike, J. Uszkoreit, and W. Feiden, "Automated nuclear segmentation in the determination of the Ki-67 labeling index in meningiomas," *Clin Neuropathol.*, vol. 25, no. 2, pp. 67-73, March - April 2006.
- [4] B. Grala, T. Markiewicz, W. Kozlowski, S. Osowski, J. Slodkaowska, and W. Papierz, "New automated image analysis method for the assessment of Ki-67 labeling index in meningiomas," *Folia Histo. Cyto.*, vol. 47, no. 4, pp. 587–592, May 2009.
- [5] V. Roullier, O. Lézoray, V. T. Ta, and A. Elmoatay, "Multi-resolution graph-based analysis of histopathological whole slide images: application to mitotic cell extraction and visualization," *Comput. Med. Imaging Graph.*, vol. 35, no. 7-8, pp. 603–615, October - December 2011.
- [6] S. Kothari, J. H. Phan, T. H. Stokes, and M. D. Wang, "Pathology imaging informatics for quantitative analysis of whole-slide images," *J. Am. Med. Inform. Assoc.*, vol. 20, pp. 1099–1108, November 2013.
- [7] S. J. Potts, D. A. Eberhard, and M. E. Salama, "Practical Approaches to Microvessel Analysis: Hotspots, Microvessel Density, and Vessel Proximity," *Methods in Pharmacology and Toxicology*, 2014, DOI: 10.1007/7653\_2014\_31
- [8] J. Molin, K. S. Devan, K. Wårdell, C. Lundström, "Feature-enhancing zoom to facilitate Ki-67 hot spot detection", *Diagnostic Pathology/Medical Imaging 2014: Digital Pathology*, March 2014.
- [9] H. Lu, T. G. Papatomas, D. van Zessen, I. Palli, R. R. de Krijger, P. J. van der Spek, W. N. M. Dinjens, and A. P. Stubbs, "Automated Selection of Hotspots (ASH): enhanced automated segmentation and adaptive step finding for Ki67 hotspot detection in adrenal cortical cancer," *Diagnostic Pathology*, vol. 9, pp. 216, November 2014.
- [10] C. Nakasu, D. H. Lim, H. Okabe, M. Nakajima, and M. Matsuda, "Significance of MIB-1 Staining Indices in Meningiomas. Comparison of Two Counting Methods," *Am. J. Surg. Pathol.*, vol. 25, no. 4, pp. 472–478, April 2001.
- [11] T. Rezanko, A. K. Akkalp, M. Tunakan, and A. A. Sari, "MIB-1 counting methods in meningiomas and agreement among pathologists," *Anal. Quant. Cytol. Histol.*, vol. 30, no. 1, pp. 47–52, February 2008.
- [12] P. Soille, *Morphological Image Analysis, Principles and Applications*. Springer: Berlin, 2003.
- [13] N. Otsu, "A threshold selection method from gray-level histograms," *IEEE Trans. Sys. Man. Cyber.*, vol. 9, no. 1, pp. 62–66, January 1979.
- [14] M. Unser, "Sum and difference histograms for texture classification," *IEEE Trans. Pattern Anal. Mach. Intell.*, vol. PAMI-8, no. 1, pp. 118–125, January 1986.
- [15] R. O. Duda, P. E. Hart, and P. Stork, *Pattern classification and scene analysis*. Wiley: New York, 2003.
- [16] B. Schölkopf and A. Smola, *Learning with Kernels. Support Vector Machines, Regularization, Optimization, and Beyond*. MIT Press: Cambridge, 2002
- [17] [<http://www.leicabiosystems.com/pathology-imaging/aperio-epathology/>], Aperio ePathology: Leica Biosystems, Nussloch, GmbH
- [18] [[www.3dhistech.com](http://www.3dhistech.com/)], 3DHISTECH Ltd.
- [19] [<http://tissuestudio.definiens.com/>], Tissue Studio 3.5: Definiens AG, Bernhard-Wicki-Straße 5, 80636 München, Germany
- [20] [[www.zeiss.com](http://www.zeiss.com)], Carl Zeiss AG